SYNTHESIS, PROPERTIES AND AC FIELD HEATING OF HYBRID NANOSTRUCTURES

Savas Delikanli, Heng Huang, Shuli He, Arnd Pralle and Hao Zeng*

Department of Physics, University at Buffalo, the State University of New York, Buffalo, NY 14260

Introduction

Nanocomposite materials demonstrate drastically altered mechanical, electric and thermal properties of their constituents. The most straightforward technique to make nanocomposites is by dispersing nanoparticles in a polymer matrix [1]. Here we report the synthesis of all-inorganic nanocomposites also called hybrid nanostructures by high temperature organic solution phase technique. They are typically formed by heterogeneous nucleation of a second component on preformed seed particles. Depending on the surface properties of different components and synthetic conditions, hybrid nanostructures with different morphologies such as core/shell, dumbbell-like and other more complicated structures can be prepared [2]. These hybrids demonstrate magnetic, semiconducting and plasmonic properties of the individual constituents and thus show multi-functionality. Moreover, these properties are often significantly modified by the neighboring components, due either to charge transfer, interface exchange coupling, or other surface and interface effects. One such example is a bimagnetic FePt/Fe_3O_4 core/shell hybrid nanoparticle [3]. Enhanced remanent magnetization and energy products have been achieved due to the strong exchange coupling between the magnetically hard and soft phases [4].

In this paper, the general synthetic strategy of hybrid nanostructures by high temperature organic solution phase technique will be presented. The physical properties of these hybrid nanostructures will be discussed. In particular, magnetic-semiconductor hybrid nanoparticles combining AC field heating and local temperature sensing will be demonstrated.

Experimental

Synthesis

Au nanoparticles were synthesized following the Brust two phase technique [5]. FePt nanoparticles were synthesized by decomposition of $Fe(CO)_5$ and reduction of $Pt(acac)_2$ by 1,2-hexadecanediol in dioctyl ether [6]. These nanoparticles were used as seeds for further growth of the hybrid nanostructures.

For the synthesis of FePt-CdS heterodimer nanoparticles, appropriate amount of CdO, oleic acid and trioctylamine were loaded into a flask. Under argon flow, the mixture was heated to 180 ˚C until a Cd-oleate complex was formed. Then, FePt seeds were injected, followed by the injection of a sulfur solution in phenyl ether. The mixture was further heated to 280 ˚C for 30 min. After cooling, the mixture was treated with ethanol followed by centrifugation and redispersion in hexane [7].

For details of the synthesis of other hybrid nanostructures, please refer to Ref. [2] and its supporting information.

Characterizations

The UV absorption spectra were collected using a Shimadzu model 3101PC UV-vis-NIR scanning spectrophotometer. The photoluminescence (PL) spectra were obtained using a Fluorolog-3 Spectrofluorometer. The nanoparticle size and morphology were characterized by transmission electron microscopy (TEM) using a JEOL model JEM-2010 microscope. The magnetic hysteresis loops were measured using a Quantum Design Physical Property Measurement System model 6000.

Results and Discussion

A schematic drawing describing the synthesis of hybrid nanostructures is shown in Fig. 1. In general, these nanostructures are obtained by seed-mediated growth, i.e. heterogeneous nucleation of a second component on preformed seed particles. The morphology is highly dependent on synthetic parameters. Polarity of the solvent strongly influences the morphology: polar solvents lead to core/shell structures while non-polar solvents lead to heterodimer nanoparticles. It is postulated that charge transfer plays a critical role in the initial heterogeneous nucleation. When a semiconductor or magnetic component nucleates on a metal such as Au seed nanoparticle, charge transfer leads to depletion of electrons in the metal component. In a nonpolar solvent, electron deficiency cannot be replenished from the surrounding medium, thus only a single nucleation can occur, resulting in heterodimers (B);

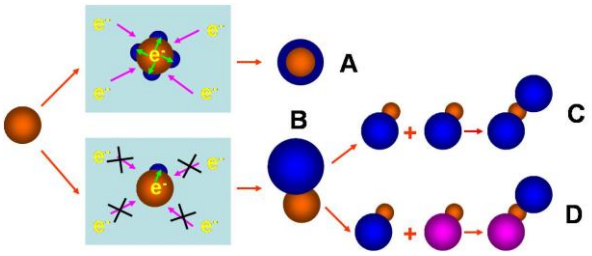

Fig.1 A schematic drawing illustrating the synthetic strategies for hybrid nanostructures: using polar solvents, heteroepitaxial nucleation and growth of a magnetic or semiconductor component on metal seed particles leads to core/shell structures (A); non-polar solvents lead to a single nucleation site resulting in heterodimer hybrids (B); fusing of two similar heterodimers leads to dumbbell-like hybrids (C); and fusing of two dissimilar heterodimers leads to ternary hybrid nanostructures (D).

in a polar solvent, on the other hand, multiple nucleation events can occur, and these nuclei eventually merge to form core/shell structures (A). More complicated morphologies can be developed from the heterodimers: two similar dimmers can fuse together under appropriate conditions to form a dumbbell-like structure (C); while two dissimilar dimmers can fuse to form a ternary nanostructure (D). Another important factor in determining morphologies is the crystal structure and lattice matching between different components. Careful examination of many high resolution TEM images of hybrid nanostructures showed matching lattices at the interface between components. Heterodimers instead of core/shell structures are formed to better relax the strain when the lattice mismatch is large. Since the strain energy scales with the aspect ratio, the semiconductor component can even cleave from the seed particle to form free nanorods [8].

Using the general synthetic strategy, we have made hybrid nanostructures with a variety of morphologies and materials combinations. For core/shell structures, we have made FePt/MFe_2O_4 (M=Fe, Co, Mn, Ni, etc), Au/MFe_2O_4, Au/Pb(Cd)Se(S), FePt/CdSe(S). For peanut-shaped heterodimers, we have prepared Au/ MFe_2O_4 and Au/Pb(Cd)Se(S). For dumbbell-like binary and ternary structures, we have synthesized MFe_2O_4/Au/MFe_2O_4, PbSe(S)/Au/PbSe(S) and MFe_2O_4/Au/PbSe(S). Selected examples of these hybrid nanoparticles are shown in Fig. 2.

These hybrid nanostructures combine magnetic, semiconducting and plasmonic properties in the same nano-entity. In many cases, the properties of individual components are modified by the conjugating ones. For example, the magnetic component often show enhanced saturation field and coercivity [2]. This is attributed to the surface anisotropy due to the modification of the electronic structure of the magnetic component at the interface. The surface plasmon resonance (SPR) frequency of

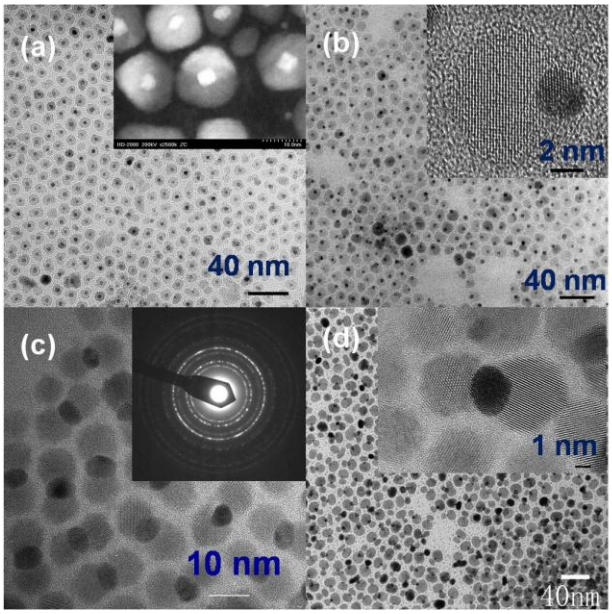

Fig. 2 TEM images of selected hybrid nanostructures: core/shell Au/Fe_3O_4 nanoparticles (inset is a dark field image) (a); Au/PbS heterodimer nanoparticles (inset is a HRTEM image) (b); Fe_3O_4-Au-Fe_3O_4 dumbbell-like hybrid nanoparticles (inset is a selected area electron diffraction pattern showing diffraction rings from both phases (c); and Fe_3O_4-Au-PbS ternary hybrid nanostructures (inset is a HRTEM image showing lattice fringes from all three components) (d).

Au component usually shows prominent red-shift in hybrids [2]. This can be mostly attributed to either the ferrite (MFe_2O_4) or semiconductor (PbSe(S)) coating that changes the dielectric environment of the metal component. The sensitivity of the SPR frequency to the dielectric environment is well-known and is the operating principle behind SPR based bio-sensing. The large dielectric constants of the ferrite or semiconducting component compared to that of vacuum or non-polar solvents cause prominent red-shift of the SPR frequencies. The IV-VI and II-VI compound semiconductors are direct band gap semiconductors. Their nanoparticles show efficient PL due to quantum confinement enhanced carrier recombination. It is interesting to observe that the PL from the metal-semiconductor hybrid structure is strongly suppressed [2]. This is a manifestation of the

interface charge transfer. The transfer of the photogenerated electrons from the semiconductor to the metal component leads to electron-hole separation, thus strongly quenches the PL. The degree of PL reduction can be tuned by the size of the metal component. The charging energy of a nanoparticle is inversely proportional to its radius. As a result the capacity of a 3 nm Au to accommodate electron transfers is much reduced from a 10 nm one. The PL of the semiconductor component is retained of a heterodimer with small metal component.

The synergistic combination of dissimilar material properties at the nanoscale can often lead to interesting applications. The bimagnetic hybrid nanoparticle with enhanced energy product as mentioned in the Introduction is one such example. It has also been shown that the metal-semiconductor hybrid nanostructure can be used for photo catalysis, due to the efficient separation of photogenerated charge carriers [9]. Here we discuss magnetic-semiconductor hybrid nanostructures for combined heating and temperature sensing. We use FePt (4 nm)/CdS (8 nm) heterodimers as an example to demonstrate the concept. The magnetic relaxation effect of FePt is used for heating in an AC magnetic field. The PL of the CdS component can then be used as a local temperature probe due to the sensitivity of the PL intensity to temperature change. Since FePt is metallic, to retain the PL intensity of the hybrids, we have chosen to work with small FePt component. As can be seen from Fig. 3(a), FePt component is superparamagnetic at room temperature, with a saturation magnetization of 400 emu/cm^3. The hybrid retains its PL, with the peak wavelength at 500 nm or 2.48 eV (Fig.3(b)), which is slightly blueshifted from the bulk value of 2.42 eV for CdS due to quantum confinement. The PL intensity of CdS is very sensitive to temperature. As can be seen from Fig. 3(c), as the temperature T increases from 293 to 308 K, a 16% reduction in integrated PL intensity is observed. The reduction is approximately linear in temperature, decreasing roughly 1% per Kelvin. This suggests that the PL of the semiconductor component can be used for local temperature sensing.

Before discussing the AC field heating results, we first establish the theoretical background and estimate the expected temperature rise. For frequencies below the ferromagnetic resonance frequency, the power loss of a magnetic nanoparticle dispersion in an AC field is mainly due to two physical mechanisms: Brownian and Néel relaxation [10]. Brownian relaxation is the relaxation due to the physical rotation of the particle. The relaxation time is given by

$$\tau_B = \frac{3\eta V_h}{k_B T} \quad (1),$$

where η is the viscosity of the medium, and V_h the hydrodynamic volume of the particle. Néel relaxation is due to the rotation of the magnetization. In the simplest Stoner-Wohlfarth model, the relaxation time is give by

$$\tau_N = \tau_0 e^{\frac{K_u V(1-\frac{H}{H_K})^2}{k_B T}} \approx \tau_0 e^{\frac{K_u V}{k_B T}} \quad (2),$$

where $1/\tau_0$ is the attempting frequency for magnetic reversal typically on the order of 10^9 Hz, K_u the uniaxial anisotropy constant, V the volume of coherent reversal, H applied field and H_K the anisotropy field. The two mechanisms operate in parallel, leading to the overall relaxation time being expressed as

$$\frac{1}{\tau} = \frac{1}{\tau_B} + \frac{1}{\tau_N} \quad (3).$$

The anisotropy and size of the particle and viscosity of the medium determines the dominating mechanism at certain frequencies. For an aqueous dispersion of FePt-CdS heterodimer nanoparticles coated with dimercaptosuccinic acid in our study, τ_B is estimated to be 3×10^{-6} s while τ_N 2×10^{-9} s, it is therefore clear that Néel relaxation plays the dominating role.

The power loss per unit volume is given by

$$P = \mu_0 \pi f {H_0}^2 \chi_0 \frac{2\pi f\tau}{1+(2\pi f\tau)^2} \quad (4).$$

One can then see that the power loss is proportional to H^2. At low frequencies P is proportional to f^2 while it saturates at higher frequencies. The susceptibility χ_0 is dependent on the shape of the minor hysteresis loop at the measuring frequency. Nevertheless it can be estimated from the DC hysteresis measurements, which shows superparamagnetic behavior as seen in Fig. 3.

The FePt/CdS heterodimer nanoparticle dispersion were loaded into an AC magnetic field of amplitude 5.0 Gauss and frequency of 40 MHz. The volumetric power loss is calculated to be 4×10^7 W/m^3. The rate of temperature rise in the aqueous dispersion (0.01 vol% concentration) is then given by $\frac{\Delta T}{\Delta t} = \frac{\mathrm{PC}}{\mathrm{C_V}}$, where C is the volume concentration and C_V the volume specific heat. $\frac{\Delta T}{\Delta t}$ is estimated to be 1 K/s.

Temperature of the dispersion was measured as a function of time and plotted in Fig. 3(d). The spurious background heating has been subtracted. The initial ramping rate is found to be 0.2 K/s. Although this is of the same order of magnitude to the theoretical value, theory significantly

overestimates the real temperature rise. This discrepancy mainly originates from the simplification of the theory which ignores the size distribution, as well as some error in concentration determination.

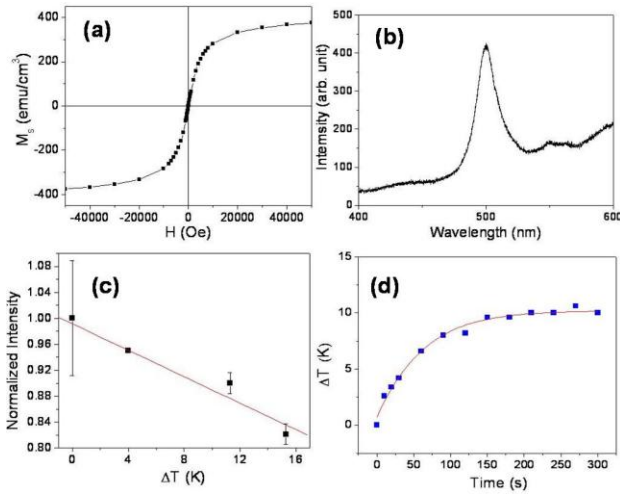

Fig. 3 Room temperature magnetic hysteresis (a) and photoluminescence (b) of FePt/CdS heterodimer nanoparticles; integrated PL intensity as a function of temperature (c); and temperature change ΔT as a function of time due to AC heating (d); dots are data points and the line is a guide to the eye.

Since magnetic nanoparticles can be used as contrast medium for MRI and magnetic hyperthermia (using heating effect of magnetic nanoparticles in an AC field to kill cancer cells), and semiconductor quantum dots can be used for bio-imaging, the magnetic-semiconductor hybrid nanostructures are promising candidates for theranostic applications (combined therapeutic and diagnosis functions). The key advantage of magnetic hyperthermia is its ability to locally heat the cancer cells without harming the surrounding area. However, to date, there is no reliable method to measure the local temperature. Because of the close proximity of the semiconductor component to the magnetic component, and because of the sensitivity of the PL intensity to temperature variations, the hybrid nanostructures we developed are ideal materials to combine cell heating and temperature sensing for this type of applications. Future work will focus on improving the SAR of the magnetic component, the shifting of PL of the semiconductor component to near IR for deeper penetration, and specific cell targeting.

Conclusion

Binary and ternary hybrid nanostructures have been synthesized by high temperature solution phase technique. They show magnetic, plasmonic and luminescent properties of the constituent components. These properties are significantly modified by the conjugating components. Synergistically integrating multiple components in nanostructures can lead to interesting applications. As an example, we showed magnetic-semiconductor hybrid nanoparticles, where the magnetic component can be used for cell heating by an AC magnetic field and the PL of the semiconductor component can be used as a local temperature probe.

Acknowledgment

Work supported by NSF DMR-0547036, UB IRDF and INSIF.

References

[1] E. Manias, "Nanocomposites - Stiffer by design," *Nature Materials*, vol. 6, pp. 9-11, Jan 2007.
[2] W. L. Shi, H. Zeng, Y. Sahoo, T. Y. Ohulchanskyy, Y. Ding, Z. L. Wang, M. Swihart, and P. N. Prasad, "A general approach to binary and ternary hybrid nanocrystals," *Nano Letters*, vol. 6, pp. 875-881, Apr 2006.
[3] H. Zeng, J. Li, Z. L. Wang, J. P. Liu, and S. H. Sun, "Bimagnetic core/shell FePt/Fe3O4 nanoparticles," *Nano Letters*, vol. 4, pp. 187-190, JAN 2004.
[4] H. Zeng, S. H. Sun, J. Li, Z. L. Wang, and J. P. Liu, "Tailoring magnetic properties of core/shell nanoparticles," *Applied Physics Letters*, vol. 85, pp. 792-794, AUG 2 2004.
[5] M. Brust, M. Walker, D. Bethell, D. J. Schiffrin, and R. Whyman, "Synthesis of Thiol-Derivatized Gold Nanoparticles in a 2-Phase Liquid-Liquid System," *Journal of the Chemical Society-Chemical Communications*, pp. 801-802, Apr 7 1994.
[6] S. H. Sun, C. B. Murray, D. Weller, L. Folks, and A. Moser, "Monodisperse FePt nanoparticles and ferromagnetic FePt nanocrystal superlattices," *Science*, vol. 287, pp. 1989-1992, Mar 17 2000.
[7] S. He, H. W. Zhang, S. Delikanli, Y. L. Qin, M. T. Swihart, and H. Zeng, "Bifunctional Magneto-Optical FePt-CdS Hybrid Nanoparticles," Journal of Physical Chemistry C, vol. 113, pp. 87-90, Jan 8 2009.
[8] W. L. Shi, Y. Sahoo, H. Zeng, Y. Ding, M. T. Swihart, and P. N. Prasad, "Anisotropic growth of PbSe nanocrystals on Au-Fe3O4 hybrid nanoparticles," *Advanced Materials*, vol. 18, pp. 1889-+, Jul 18 2006.
[9] P. V. Kamat, "Meeting the clean energy demand: Nanostructure architectures for solar energy conversion," *Journal of Physical Chemistry C*, vol. 111, pp. 2834-2860, Feb 22 2007.
[10] R. E. Rosensweig, "Heating magnetic fluid with alternating magnetic field," *Journal of Magnetism and Magnetic Materials*, vol. 252, pp. 370-374, Nov 2002.

*e-mail: haozeng@buffalo.edu